10

Maximum Power Point Tracker Applied in Batteries Charging with Photovoltaic Panels

José António Barros Vieira[1] and Alexandre Manuel Mota[2]
[1]*Instituto Politecnico de Castelo Branco, Escola Superior de Tecnologia de Castelo Branco, Departamento de Engenharia Electrotécnica*
[2]*Universidade de Aveiro, Departamento de Electrónica Telecomunicações e Informática, Instituto de Engenharia Electrónica e Telemática de Aveiro*
Portugal

1. Introduction

Recently, the concern for environmental issue has been rising in the world such as global warming by exhausting carbon dioxide (CO2) and breaking of ozone layer by freon gas. On December 1997, during the Kyoto Conference on Climate Change (COP3), it was agreed that by the year 2012 the developed countries would reduce at least 5% of the green house gases compared with year 1990 (Riza et al., 2003). Moreover, the global energy shortage and the need for sustainable energy systems enforce the development of power supply structures that are based mainly on renewable resources.

Photovoltaic (PV) system is gaining increased importance as a renewable source due to advantages such as the absence of fuel cost, little maintenance and no noise and wear due to the absence of moving parts. But there are still two principal barriers to the use of photovoltaic systems: the high installation cost and the low energy conversion efficiency.

A PV panel is a non-linear power source, i.e. its output current and voltage (power) depends on the terminal operating point. The maximum power generated by the PV panel changes with the intensity of the solar radiation and the operating temperature. To increase the ratio output power/cost of the installation it is important that PV panel operates in the maximum output power point (MPP).

This chapter describes a lead acid battery charger using a PV panel with high efficiency. It starts by introducing the PV panel characteristics and describing the DC/DC converter need to implement the MPPT algorithm. This is the most important part of this work and shows how to charge and discharge correctly a lead acid battery.

The developed prototype uses the perturbation and observation (P&O) MPPT algorithm with the objective to maximize energy storage in the battery. The MPPT algorithm is integrated in one of the main stages of charge of lead-acid batteries making an autonomous and intelligent system that can be used to feed any remote load or small application. It is very important to respect the correct battery charge curves because it will prolong its correct operation and live (Vieira and Mota, 2009).

The P&O MPPT algorithm is used to control the maximum transfer power from a PV panel to the battery. This algorithm is executed by a microcontroller using the PV voltage and

current measurements to define the duty cycle of a pulse width modulation signal applied to the DC/DC converter. The schematic and design of the DC/DC converter are explained. The DC/DC converter used is of the SEPIC topology because it easily adapts any PV output voltage to any battery input voltage.

One of the most frequently used MPPT methods is the perturbation and observation algorithm, although this algorithm has some converging problems with rapidly insolation changes. This problem can be solved using the solution presented in (Sera et al., 2006). In this work, PV voltage and current are measured in the middle of the sampling interval, making possible to determine if the verified changes are due to perturbation algorithm or to shadows that cover the PV panel. Another popular MPPT algorithm is the incremental conductance method (IncCond) (Hussein et al., 1995). The authors developed the incremental conductance MPPT algorithm avoiding the drawbacks of the P&O MPPT algorithm. It is based on the fact that the derivative of the output power P with respect to the panel voltage V is equal to zero at the MPP. The solar panel's P-V characteristics presented in figure 2 show further that the derivative is greater than zero to the left of the MPP and less than zero to the right of the MPP. This algorithm shows that enough information is gathered to determine the relative location of the MPP by measuring only the incremental and instantaneous panel conductance's dI/dV and I/V, respectively.

In this work, perturbation and observation MPPT algorithm was chosen, due to its simplicity and to its low computational power needs (Knop, 1999).

To implement a correct charger for a lead-acid battery, the correct charge curves are presented and the four charging stages are described. This work also explains that if the correct charge curves are respected in the charge periods the correct operation period of time of the lead acid battery will be longer. In the developed system only two of the four charging stages are implemented. The first stage is avoided by the discharge supervisor implemented algorithm and the fourth stage is made extending the third stage. The discharge supervision algorithm simply monitors the battery voltage and if it goes bellow a minimum value the load is disconnected waiting for a new charge.

Finally, experimental results of the performance of the designed P&O MPPT algorithm, corresponding to the 2º stage of lead acid battery charge, are presented and compared with the results achieved with the direct connection of the PV panel to the battery.

The remainder of this chapter is organized as follows: section 2 presents the photovoltaic panel characteristics, section 3 presents the DC/DC SEPIC schematic and design, section 4 shows the perturbation and observation maximum power point tracking algorithm. Section 5 presents the algorithm proposed to the different stages of the lead-acid battery charging process, section 6 shows the implemented prototype board, section 7 discuss the experimental results of charging with the P&O MPPT algorithm and with out it, ending with the conclusions presented in section 8.

2. Solar array characteristics

The maximum power point of a solar panel changes in accordance with changes in the solar irradiance intensity, angle and panel temperature. The typical characteristic curves of current versus voltage, power versus voltage at different levels of solar irradiation and power versus voltage at different temperatures, are illustrated in figure 1, figure 2 and figure 3 respectively.

Figure 1 illustrates the operating characteristic of the panel under several given solar insolations. It consists of two regions: one is the current source region, and the other is the voltage source region. In the voltage source region, the internal impedance of the panel is low. That region is the right side of the current-voltage curve. The current source region, in which the internal impedance of the panel is high, is at the left side of the current-voltage curve. The MPP of the panel is located at the knee of the current-voltage curve. According to the maximum power transfer theory, the power delivered to the load is maximum when the source internal impedance matches the load impedance. Thus, the impedance seen from the converter input side (can be adjusted by PWM control signal) needs to match the internal impedance of the panel if the system is required to operate at or near the MPP of the solar array. If the system operates on the voltage source region (namely low impedance region) of panel characteristic curve, the panel terminal voltage will collapse (Hua & Lin, 2003).

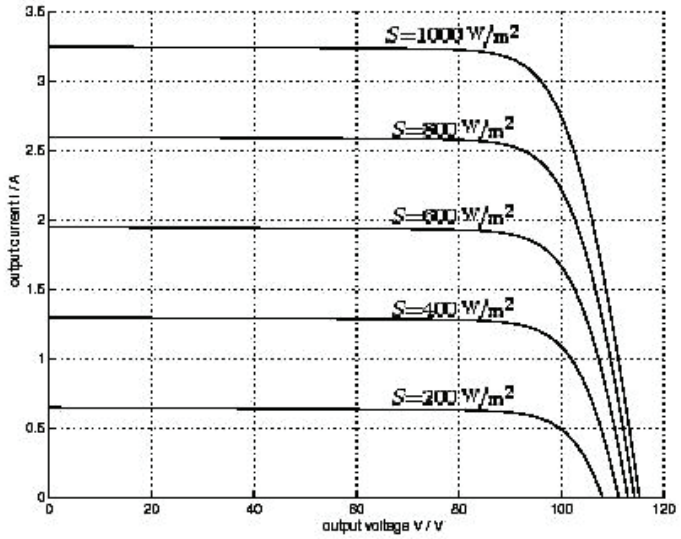

Fig. 1. I-V characteristics of a photovoltaic panel for different values of irradiance S at a temperature of 25 ºC.

From figure 2 and Figure 3, it can be observed that each curve has a maximum power point, which is the optimal point for the efficient use of the panel. This point depends of the values of irradiance and working temperature. The main function of a MPPT is to adjust the panel output voltage to a value which the panel supplies the maximum energy to the load (Torres, 1998).

Thus, a DC/DC converter will be used to match the source internal impedance with the load impedance achieving the MPP. The applied MPPT algorithm will be explained in detailed in section 4.

3. DC/DC SEPIC converter

To implement the P&O MPPT algorithm a SEPIC (Single-Ended Primary Inductance Converter) is used. This DC/DC type of converter is an increasingly popular topology,

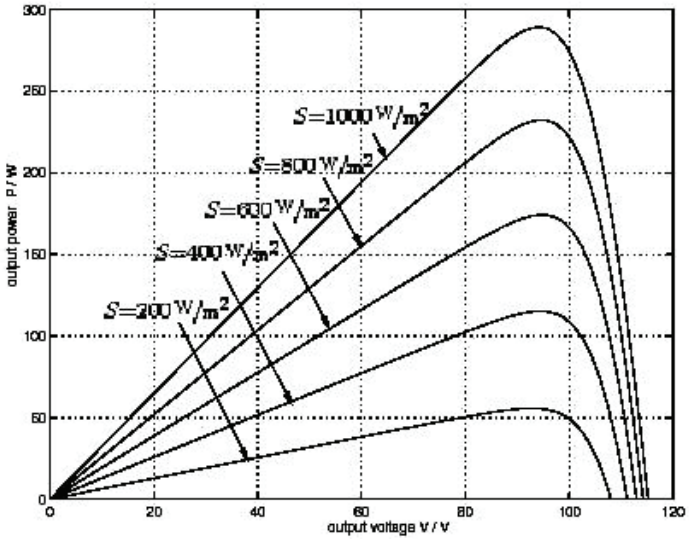

Fig. 2. P-V characteristics of a photovoltaic panel for different values of irradiance S at a temperature of 25 °C.

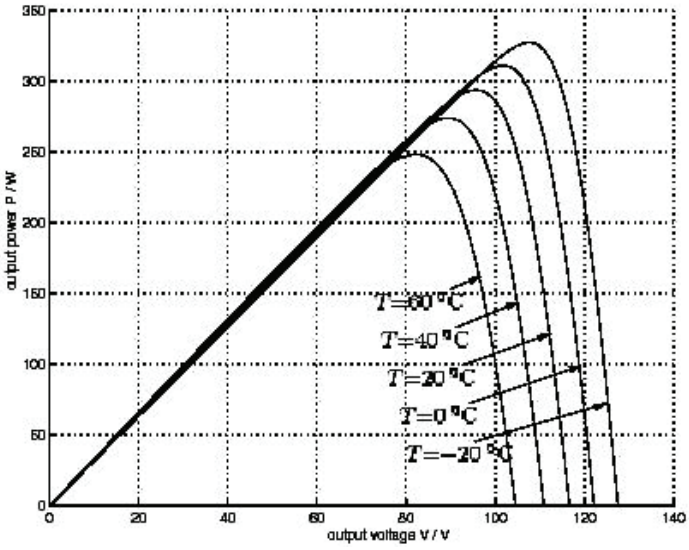

Fig. 3. P-V characteristics of a photovoltaic panel for different values of temperature T at irradiance of 1000W/m².

particularly in battery powered applications, because the input voltage can be higher or lower than the output voltage. This topology presents obvious design and working advantages. In this work, for the implementation of the maximum power point tracker the SEPIC, working in continuous conduction mode, is used as the power-processing unit. The PWM is controlled with a switching frequency of 125 kHz that actuates the Mosfet switch M1. The power flow is controlled by adjusting the on/off duty-cycle. Figure 4 shows the schematic of the DC/DC converter implemented. It has one Mosfet, one diode, two inductances and tree capacitors.

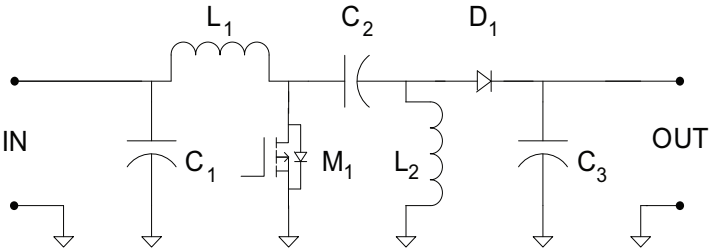

Fig. 4. SEPIC DC/DC converter circuit.

Using a PV panel with the following characteristics: maximum power P_{max}=9.31 W, maximum voltage V_{mp}=17.4 V, maximum current I_{mp}=0.54 A, open circuit voltage V_{oc} = 21.2 V, short-circuit current I_{cc}=0.66 A, the DC/DC converter design starts with the selection of the two separate inductors L_1 and L_2. For a general working point with:

Input voltage (V_{in})	12V – 16V
Output (V_{out} & I_{out})	12V, 0.6A
Switching frequency (F_s)	125kHz
Expected efficiency	90%

First it is need to calculate the duty cycle; $D = V_{out}/(V_{out} + V_{in})$; The worst case condition for inductor ripple current is at maximum input voltage so; $D = 12/(12 + 16) = 0.429$;
Calculating the value of L_2:

$$V = L\, di/dt \tag{1}$$

Where V is the voltage applied to the inductor, L in the inductance, di is the inductor peak to peak ripple current and dt is the duration the voltage applied. Hence:

$$L = V.dt/di \tag{2}$$

$$dt = 1/F_s \times D \tag{3}$$

$$dt = 1/(125 \times 10^3) \times 0.428 = 3.42\ \mu s \tag{4}$$

$V = V_{in}$ during the switch ON time so:

$$L_2 = 16 \times (3.42 \times 10^{-6}/0.4) \tag{5}$$

$$L_2 = 136.8\ \mu H \tag{6}$$

Using the nearest preferred value would lead to the selection of a 150 µH inductor. It is common practice to select the same value for both input and output inductors in SEPIC designs although when two separate parts are being used it is not essential.
Having selected the inductance value we now need to calculate the required RMS and peak current ratings for both inductors. For input inductor L_1:

$$I_{rms} = (V_{out} \times I_{out})/(V_{in}\,(min) * efficiency) \quad (7)$$

$$I_{rms} = (12 \times 0.6)/(12 \times 0.9) = 0.667A \quad (8)$$

$$I_{peak} = I_{rms} + (0.5 \times I_{ripple}) \quad (9)$$

Although worst case ripple current is at maximum input voltage the peak current is normally highest at the minimum input voltage.

$$I_{ripple} = (V.dt)/L \quad (10)$$

$$I_{ripple} = (12 \times 3.42 \times 10^{-6})/\ 150 \times 10^{-6} = 0.27A \quad (11)$$

$$I_{peak} = 0.667 + 0.135 = 0.804A \quad (12)$$

So a 150µH, 0.667Arms and 0.804Apk rated inductor is required. For the output inductor L_2:

$$I_{rms} = I_{out} = 0.6A \quad (13)$$

$$I_{ripple} = (16 \times 3.42 \times 10^{-6})/\ 150 \times 10^{-6} = 0.365A \quad (14)$$

$$I_{peak} = 0.6 + 0.182 = 0.782A \quad (15)$$

So a 150µH, 0.6Arms and 0.782Apk rated inductor is required.
Finally, the SEPIC components used are:

	with I_{sat} = 4.0A because if V_{in} = 6V I_{rms}
L_1 = 150µH and L_2 = 150µH	will be near to the double of the calculated current for V_{in} = 12V
C_1 = 47 µF, C_2 = 47µF ,C_3 = 47µF	with V_{max} = 40V
M_1 of I_{max} = 4.0A	switching Mosfet at 125kHz
D_1 of I_{max} 4.0A	Schotkky Diode

4. The P&O maximum power point tracker algorithm

The P&O MPPT is one of the so called 'hill-climbing' methods, which are based on the fact that in case of the V-P characteristic, on the left of the MPP the variation of the power against voltage dP/dV > 0, while at the right, dP/dV < 0 (Weidong & Dunford, 2004).
In Figure 2, if the operating voltage of the PV panel is perturbed in a given direction and dP/dV > 0, it is known that the perturbation moved the panel's operating point toward the MPP. The P&O algorithm would then continue to perturb the PV panel voltage in the same direction. If dP/dV < 0, then the change in operating point moved the PV panel away from the MPP, and the P&O algorithm reverses the direction of the perturbation (Hohm & Ropp, 2000).

The main advantage of the P&O method is its implementation simplicity and its low computational demand. However it shows some limitations, like oscillations around the MPP in steady state operation, slow response speed, and tracking in wrong way under rapidly changing atmospheric conditions (Hohm & Ropp, 2000), (Femia et al., 2004), (Brambilla et al., 1999). To reduce the presented limitations it will be useful to use a small sampling rate. In this work it was used a sampling rate of 100 ms.
Using a SEPIC with current and voltage resistance sensors illustrated in Figure 5, the P&O MPPT algorithm was implemented. The algorithm needs only the PV voltage and current information to work correctly, the battery voltage and current information will be used to control the battery charging stages and supervise its discharge.

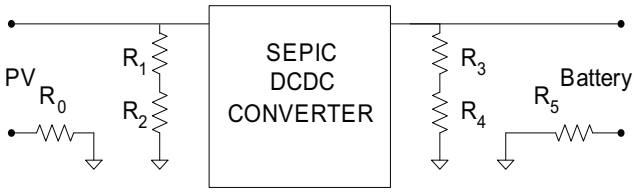

Fig. 5. Voltage and current resistive sensors for MPPT and battery charging algorithm.

R_0=R_5=0.01Ω for current measurements and R_1=R_3=910kΩ and R_2=R_4=150kΩ for voltage measurements.
The flow chart of the P&O MPPT implemented algorithm is illustrated in figure 6. The parameter K is the step given to the PWM signal. This parameter can vary depending of the working point of the DC/DC converter. To get a faster convergence we need big K values and to avoid big oscillations near to the MPPT working point we need small K values.
The P&O MPPT control algorithm is implemented in a microcontroller (ATTINY861V) that has ten 10-bits analogue-to-digital (A/D) converters and two fast PWM mode signals with 10-bits of resolution. The control circuit compares the PV output power before and after a change in the duty-cycle of the DC/DC converter control signal and acts in conformity. It is expected that the algorithm shows a small constant oscillation in the MPP working point inherent to the is working principle. The PWM_old is the sample of the PWM signal in the previous iteration of the algorithm and ΔP_{PV} is the variation of the delivered power to the battery.

5. Battery charging algorithm

The complete battery charging demands a complex control strategy, in which it would be possible to charge the battery, between its limits, in the faster possible way because the daily period of energy generation of the PV panel is limited (Galdino & Ribeiro, 1994).
To achieve a fast, safe and complete battery lead-acid charge, some of the manufacturers recommend dividing the charging process in four stages that are designated by: (i) trickle charge, (ii) bulk charge, (iii) over charge and (iv) float charge (Hesse, 1997) and (Rosemback, 2004). Figure 7 show the curves of current and voltage applied to the battery during a correct charging cycle.

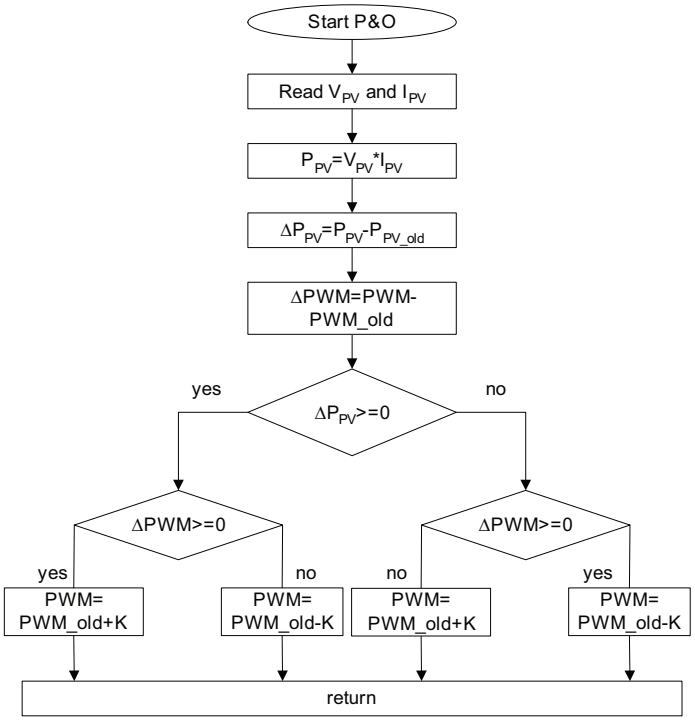

Fig. 6. P&O MPPT algorithm.

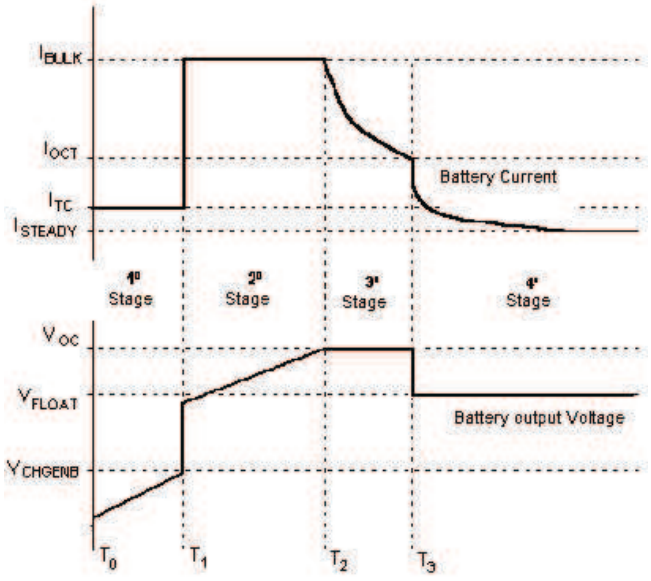

Fig. 7. Current and voltage curves in the four stages of battery charge.

5.1 Trickle charge - 1º stage (from T0 to T1)

This first stage is active when the battery voltage is below the value $V_{CHGENB.}$ This voltage value, specified for the manufacturers, shows that the battery arrives at its critical discharge capacity. In this condition the battery should receive a small charge current defined by I_{TC} that has a typical value of C/100 where C is the normal battery capacity with a 10 hours charging process.

This small current I_{TC} is applied until the battery voltage reaches the value of V_{CHGENB}. This stage also avoids that some accident could happens in the case of the one battery element is in curt circuit, therefore if this really happens the battery voltage will not grow and then the battery charging process does not pass to the next stage.

5.2 Bulk charge - 2º stage (from T1 to T2)

After the battery voltage reaches the value V_{CHGENB} it should be applied to the battery a constant current I_{BULK}. The I_{BULK} is the maximum charge current that battery supports without a big water losing, and its value is specified by the manufacturers. This current is applied until the battery voltage reaches the maximum value of over charge voltage, defined by V_{OC}, and also specified by the manufacturers. In this stage the prototype implemented board will run the P&O MPPT algorithm but the I_{BULK} is never exceeded. The maximum power of the PV panel should be correctly chosen.

5.3 Over charge - 3º stage (from T2 to T3)

During this stage the control algorithm should regulate the battery voltage V_{OC} until the complete charge has been reached. When the charging current fall down to a pre-established value I_{OTC} and the voltage stays in the value V_{OC}, the charge process should go to the next, and final, stage. The value of I_{OCT} is around 10% of the I_{BULK}.

5.4 Float charge - 4º stage (from T3 until the end)

In this stage the control algorithm will apply to the battery a constant voltage V_{FLOAT} which is specified by the battery manufacturers. This voltage is applied to the battery with the objective of avoiding its auto-discharge. During the discharging process the battery voltage will fall down and when it reaches 0.9 V_{FLOAT} the control algorithm will execute again the 2º stage providing the I_{BULK} current.

The control algorithm only returns to the 2º stage if the PV panel is capable of delivering energy. If it is not the case the battery will continue the discharge process. If the voltage goes below the value V_{CHGENB} the control algorithm should restart the charging process in 1º stage as soon as the PV panel is capable of delivering energy.

In this work some simplifications have been introduced in the implementation of the four different charging stages of a lead-acid battery. The 1º stage was not implemented because the discharge batteries voltage, with this prototype board, does not go below V_{FLOAT}. The possible applied load is disconnected from the battery by the control algorithm avoiding reaching the critical discharge.

The 4º stage was not implemented but the 3º stage is continued until the charge current reach I_{STEADY} and finally the charging process is ended. When the PV panel has energy to delivery and the battery voltage is below the V_{OC}, the control algorithm executes the 2º stage.

The battery charging algorithm can be seen in figure 8. Values V_b and I_b are the battery voltage an delivered current and T_b is the battery temperature. The maximum value of the V_{OC}

depends of the battery temperature. The temperature of the battery T_b is measured using a NTC temperature sensor and its linearisation is made in software using a conversion table.
From figure 8 it is clear that only the 2º and the 3º stages are implemented from the four stages proposed in (Hesse, 1997) and (Rosemback, 2004).

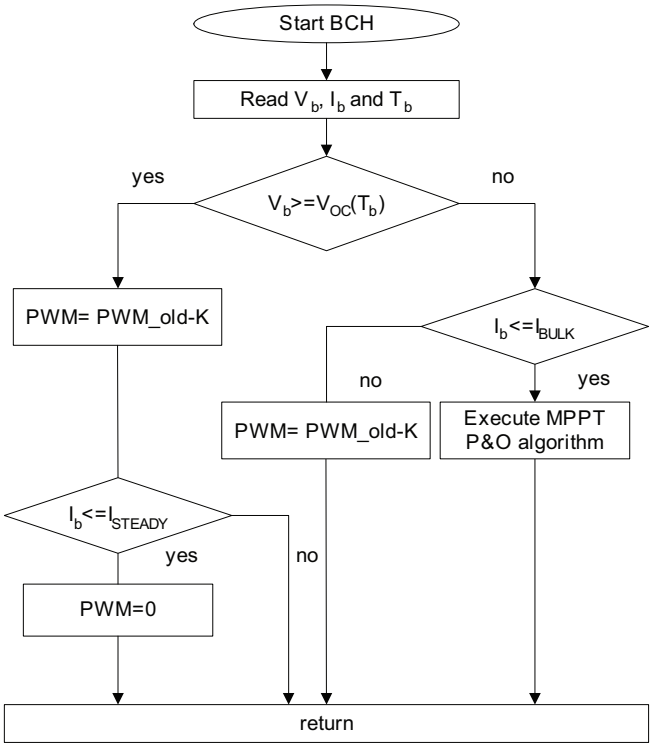

Fig. 8. Battery charging algorithm with two main stages.

6. Implemented prototype board

The implemented prototype board is illustrated in figure 9. It can be seen the PV panel connection in the right side of the photo (IN) and the connection to the battery (B) and to the possible load (L) both in the left side.
The described charging process of lead-acid batteries is executed with the P&O MPPT algorithm integrated to make an autonomous system that can be used to feed any autonomous load application. This board is also prepared to feed led light autonomous signalisation systems and could be used in any other remote small application.
The board also monitors the discharge of the battery. There is a minimum battery voltage, depending of the battery temperature, that shouldn't be over crossed. If that happens the system disconnects the load until a new charge.

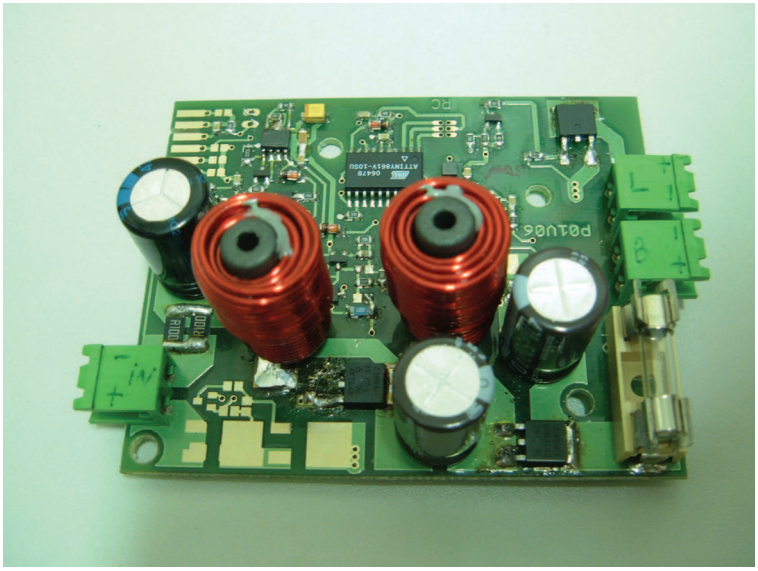

Fig. 9. Photo of the MPPT and battery charger prototype board.

7. P&O MPPT experimental results

The experimental results of battery charging using the P&O MPPT algorithm are divided in two separated tests each one divided in two phases. In the first phase the Photo Voltaic panel is directly connected to the battery element (first 85 samples) and in the second phase the panel is connected to the battery element using the developed board running the P&O MPPT algorithm (from samples 85 to the end).

In the first test a PV panel with a Pmax = 9.31 W (Vmp = 17.4 V, Imp = 0.54 A) connects to one lead-acid battery of V = 12 V (Imax = 7.5 Ah). In the second test the same PV panel is connected to a bank of four lead-acid batteries of V = 6 V (Imax = 1.8 Ah) connected in parallel. The tests results are illustrated in figures 10 and 11.

From first test it can be seen that charging the 12V battery with the direct connection of the PV panel to the battery, the absorbed power from the PV panel is around 7W and with the P&O MPPT algorithm the absorbed power from the PV panel is around 8W. The MPPT algorithm presents small oscillations around the maximum power point as expected. The algorithm takes about 60 samples to go from zero to the maximum power point.

From the second test results it can be seen that with the direct connection of the PV panel to the bank of four batteries the absorbed power from the PV panel is around 4.5W and charging the batteries with the P&O MPPT algorithm, corresponding to the second charge stage, the absorbed power from the PV panel is around 7.5W. The algorithm takes about 40 samples from zero to the maximum power point.

The experimental setup using the P&O MPPT always gives more delivered energy to the battery than the direct connection. The P&O MPPT has increased the PV panel capacity of supply energy in 12.5% using a 12V battery and 40% using four 6V batteries connected in parallel.

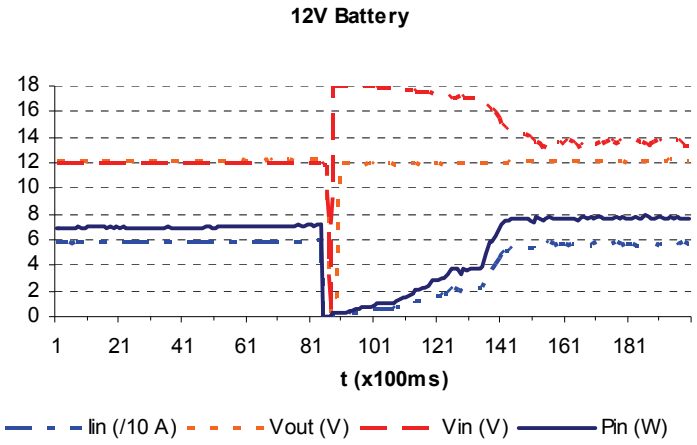

Fig. 10. Experimental results of the P&O MPPT algorithm power with a 12V battery (first phase direct connection and second phase using the developed board).

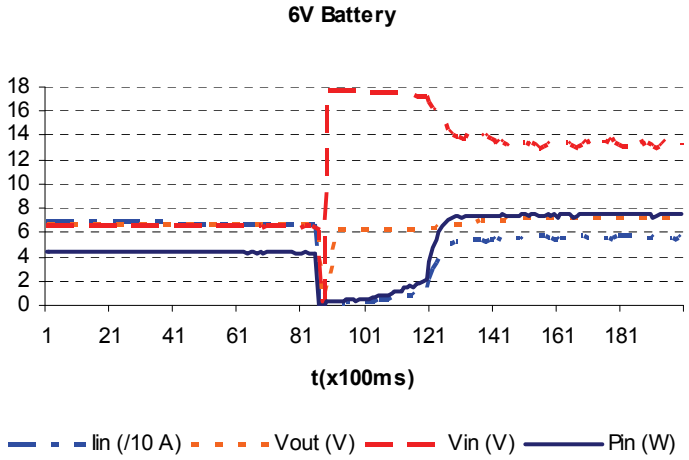

Fig. 11. Experimental results of the P&O MPPT algorithm power with four 6V batteries (first phase direct connection and second phase using the developed board).

8. Conclusions

This work presents a prototype board based in a small microcontroller that controls the lead acid battery charging process and also the correct use of the lead-acid battery supervising its discharge. The control algorithm executes the P&O maximum power point tracking function allowing, according to solar irradiance and temperature, transfer the maximum energy generated by photovoltaic panel to the battery. This P&O algorithm increase the efficiency power transference in comparison to systems that have not a MPPT (direct connection),

reducing the size and the cost of the PV panel. The use of a SEPIC converter has some advantages because it easily adapts any PV output voltage to any input battery voltage as showed in the presented experiments.

This board enables the fast, safe and complete battery lead-acid charging process and also monitor its discharge. For future work the complete charging process should be analysed to compare with another system working with out P&O MPPT algorithm. From these results it is expect that the charging process using the MPPT algorithm will be faster and more efficient. These results will prolong for more time the correct operation of the lead acid battery.

For future work, it would be interesting to apply the P&O MPPT algorithm to a thermal solar panels to absorb the maximum thermal power from the irradiated solar energy. The thermal energy could be transferred to water tanks for future utilizations for domestic or industrial use. To implement this system we will need the measurement of the water flow and increase of the temperature of the water (output subtracted to input temperatures of the water of the thermal solar panel) to calculate the water thermal power that is the product of the two referred measurements. Finally, with the control of the water flow it should be possible to impose the MPP in a solar thermal system optimizing the efficiency of the thermal energy transference.

9. References

Brambilla A., Gambarara M., Garutti A. and Ronchi F.(1999). New Approach to Photovoltaic Arrays Maximum Power Point Tracking. *Proceedings of Power Electronics Specialists Conference, PESC 99*, vol. 2, pp 632–637, 27 June-1 July 1999.

Femia N., Petrone G., Spagnuolo G. and Vitelli M. (2004). Optimizing Sampling Rate Of P&O MPPT Technique, *Proceedings of Power Electronics Specialists Conference, PESC04*, vol. 3, pp 1945-1949, 20-25 June 2004.

Galdino M. A. E., Ribeiro C. M. (1994). An Intelligent Battery Charge Controller for Small Scale PV Panel, *Proceedings of 12th European Photovoltaic Solar Energy Conference and Exhibition*, 1994.

Hesse K. (1997). An Off-Line Lead -Acid Charger Based on the UC3909, *Technical report*, Unitrode Company, 1997.

Hohm D.P, Ropp M. E. (2000). Comparative Study of Maximum Power Point Tracking Algorithms Using an Experimental, Programmable, Maximum Power Point Tracking Test Bed, *Proceedings of Photovoltaic Specialists Conference,* Conference Record of the Twenty-Eighth IEEE, pp 1699 – 1702, 15-22 Septembre 2000.

Hua C. and Lin J. (2003). An On-Line MPPT Algorithm for Rapidly Changing Illuminations of Solar Arrays, *Proceedings of Renewable Energy*, vol. 28, pp 1129–1142, 2003.

Hussein K. H., Muta I., Hoshino T. and Osakada M. (1995). Maximum Photo- Voltaic Power Tracking: an Algorithm for Rapidly Changing Atmospheric Conditions, *In IEE Proceedings Generation, Transmission and Distribution*, vol. 142(1), pp 59-64, IEE Steven age, Herts, U.K., January, 1995.

Knop H. (1999). *Analysis, Simulation, and Evaluation Of Maximum Power Point Tracking (MPPT) Methods for a Solar Powered Vehicle*, Mater of Science Thesis in Electrical and Computer Engineering, Portland State University, 1999.

Riza M., et al. (2003). A Maximum Power Point Tracking For Photovoltaic-Spe System Using A Maximum Current Controller, *Proceedings of Solar Energy Materials & Solar Cells*, vol.75 , pp 697–706, 2003.

Rosemback R. H. (2004). *Conversor Cc-Cc Bidirecional Buck-Boost Atuando Como Controlador De Carga De Baterias Em Um Sistema Fotovoltaico*, Mater of Science Thesis in Electrical Engineering, University Federal de Juiz de Fora, 2004.

Sera D., Kerekes T., Teodorescu R., and Aalborg F. Blaabjerg (2006). Improved MPPT Method For Rapidly Changing Environmental Conditions, *IEEE International Symposium on Industrial Electronics*, vol. 2, pp 1420 – 1425, 9-13 July, 2006.

Torres A. M. (1998). *Aproveitamento Fotovoltaico Controlado por Redes Neurais Artificiais Interligado ao Sistema Elétrico*, MSc Thesis, GPEC – DEE – UFC, Septembre, 1998.

Weidong X., Dunford W.G. (2004). A Modified Adaptive Hill Climbing MPPT Method For Photovoltaic Power Systems, *Proceedings of Power Electronics Specialists Conference PESC 04*, vol. 3, 20-25, pp 1957–1963, June 2004.

Vieira J. A., Mota A. M. (2009). Maximum Power Point Tracker Applied in Batteries Charging with Thermoelectric Generator Using the Waste Energy from a Gas Water Heater, *Proceedings of the Conference on Control Applications*, St. Petersburg, Russia, vol. 1, pp. 1477-1482, July 2009.

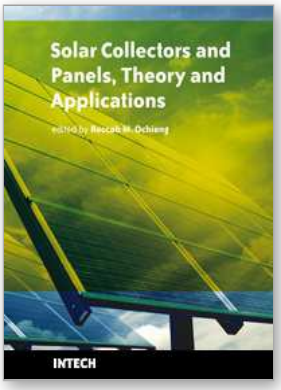

Solar Collectors and Panels, Theory and Applications

Edited by Dr. Reccab Manyala

ISBN 978-953-307-142-8
Hard cover, 444 pages
Publisher Sciyo
Published online 05, October, 2010
Published in print edition October, 2010

This book provides a quick read for experts, researchers as well as novices in the field of solar collectors and panels research, technology, applications, theory and trends in research. It covers the use of solar panels applications in detail, ranging from lighting to use in solar vehicles.

How to reference

In order to correctly reference this scholarly work, feel free to copy and paste the following:

Alexandre Mota and José Vieira (2010). Maximum Power Point Tracker Applied to Charging Batteries with PV Panels, Solar Collectors and Panels, Theory and Applications, Dr. Reccab Manyala (Ed.), ISBN: 978-953-307-142-8, InTech, Available from: http://www.intechopen.com/books/solar-collectors-and-panels--theory-and-applications/maximum-power-point-tracker-applied-to-charging-batteries-with-pv-panels

INTECH
open science | open minds

InTech Europe
University Campus STeP Ri
Slavka Krautzeka 83/A
51000 Rijeka, Croatia
Phone: +385 (51) 770 447
Fax: +385 (51) 686 166
www.intechopen.com

InTech China
Unit 405, Office Block, Hotel Equatorial Shanghai
No.65, Yan An Road (West), Shanghai, 200040, China
中国上海市延安西路65号上海国际贵都大饭店办公楼405单元
Phone: +86-21-62489820
Fax: +86-21-62489821